coatings

MDPI

Article

A Cellular Automata-Based Model for Simulating the Chloride Ion Diffusion Process of Concrete with Admixtures

Jingnan Ding [1,2,*], Yexuan Zhou [1], Jinsong Zhu [3,4,*], Qingling Meng [5] and Ankai Cao [6]

[1] School of Civil Engineering, Shandong Jianzhu University, Jinan 250101, China
[2] Key Laboratory of Building Structural Retrofitting and Underground Space Engineering, Ministry of Education, Shandong Jianzhu University, Jinan 250101, China
[3] School of Civil Engineering, Tianjin University, Tianjin 300072, China
[4] Key Laboratory of Coast Civil Structure Safety, Ministry of Education, Tianjin University, Tianjin 300072, China
[5] Civil Engineering College, Tianjin Chengjian University, Tianjin 300384, China
[6] State Grid Shandong Integrated Energy Services Co., Ltd., Jinan 250101, China
* Correspondence: dingjingnan23@sdjzu.edu.cn (J.D.); jszhu@tju.edu.cn (J.Z.)

Abstract

To accurately simulate the chloride ion diffusion process in concrete containing mineral admixtures under coupled multi-factor effects, a cellular automata (CA)-based numerical model is developed to predict the chloride ion concentration at different depths and exposure times. The proposed model incorporates the influences of spatiotemporal variability, stress state, and admixture replacement ratio into the evolution rules of chloride transport. Accordingly, the time-dependent chloride diffusion coefficient is modified to account for the effects of fly ash and slag, enabling a more realistic representation of chloride transport behavior in admixture-modified concrete. Long-term field exposure test data reported in the literature are adopted to validate the proposed model. The simulated chloride concentration profiles at various depths and exposure durations show good agreement with experimental measurements, particularly at medium-to-long exposure ages. The results demonstrate that the CA model provides a reasonable and effective way for simulating chloride ion ingress in concrete with mineral admixtures. Furthermore, under comparable strength conditions, an increase in slag replacement ratio leads to enhanced resistance against chloride ion ingress, highlighting the significant role of mineral admixtures in improving the durability performance of concrete structures.

Keywords: fly ash; slag; concrete; chloride ion diffusion; cellular automata

Check for updates

Academic Editor: Edoardo Proverbio

Received: 12 February 2026
Revised: 2 March 2026
Accepted: 6 March 2026
Published: 8 March 2026

Copyright: © 2026 by the authors. Licensee MDPI, Basel, Switzerland. This article is an open access article distributed under the terms and conditions of the Creative Commons Attribution (CC BY) license.

1. Introduction

Reinforced concrete structures exposed to marine environments, deicing salts, and saline soils are particularly vulnerable to chloride-induced deterioration, which has been identified by numerous studies as one of the principal causes of durability degradation and service life reduction [1]. Chloride ions penetrate concrete mainly through diffusion, capillary suction, and permeation processes, and when the chloride concentration at the steel surface exceeds a critical threshold commonly reported in the literature, the passive film is destroyed, initiating reinforcement corrosion and subsequent cracking, spalling, and loss of structural capacity. Therefore, accurate characterization and prediction of chloride ion diffusion behavior in concrete is essential for durability-oriented design and life-cycle assessment of concrete structures.

Extensive experimental and theoretical investigations have shown that chloride ion transport in concrete is a highly complex and non-stationary process governed by multiple interacting factors, including material composition, pore structure, environmental conditions, and mechanical actions. Traditionally, the diffusion behavior of chloride ions has been described using Fick's second law, in which the apparent diffusion coefficient is regarded as a key parameter characterizing the resistance of concrete to chloride ingress. Despite its effectiveness in many practical applications, numerous studies have demonstrated that parameters such as the water–binder ratio, curing age, temperature, humidity, stress state, and wet–dry cycling significantly influence the effective diffusion coefficient and the resulting chloride concentration profiles [2,3]. Under sustained or cyclic mechanical loading, the evolution of microcracks alters the connectivity of pore networks, leading to nonlinear variations in chloride diffusivity [4]. Experimental results indicate that compressive stress may reduce chloride diffusivity at relatively low stress levels by compacting the pore structure, whereas tensile stress and multiaxial loading conditions tend to accelerate chloride ingress due to crack initiation and propagation [5]. In addition, under alternating humidity conditions, wet-dry cycles, or salt-spray environments, the coupling between moisture transport and chloride diffusion further complicates the ingress process, resulting in pronounced time-dependent and spatially non-uniform characteristics [2]. At the structural scale, macroscopic chloride transport models and service-life-oriented assessment frameworks have been developed to bridge material-level chloride diffusion behavior and long-term durability performance of concrete structures in marine environments [3,6,7].

In recent decades, mineral admixtures such as fly ash, slag, silica fume and waste glass powder have been widely incorporated into concrete to improve durability and sustainability. Previous studies have reported that mineral admixtures can enhance the resistance of concrete to chloride ion penetration through a combination of physical and chemical mechanisms. On the one hand, pozzolanic reactions consume calcium hydroxide and generate additional C-S-H gel, resulting in pore refinement and reduced pore connectivity. On the other hand, alumina-rich phases in certain admixtures promote the formation of chloride-binding products, such as Friedel's salt, thereby reducing the concentration of free chloride ions available for transport [8,9]. Experimental studies on high-performance concrete incorporating fly ash and silica fume have shown a marked reduction in apparent chloride diffusion coefficients with increasing curing age [4]. Similar improvements have been reported for slag-blended concrete and recycled aggregate concrete, although the inherent heterogeneity of these materials leads to more pronounced spatial variability in chloride transport behavior [2]. These results indicate that mineral admixtures not only modify the average transport properties of concrete but also increase the complexity and heterogeneity of chloride diffusion pathways.

Conventional chloride diffusion models based on Fick's law generally treat concrete as a homogeneous and continuous medium. Although time-dependent diffusion coefficients and multi-physics coupling approaches have been proposed, the discrete nature of concrete microstructure, local material variability, microcrack evolution, and localized chloride binding effects are still difficult to adequately represent within a purely continuum framework, particularly for concrete incorporating mineral admixtures and subjected to multi-factor coupled actions [10].

To address these limitations, cellular automata (CA) methods have been introduced as an alternative numerical approach for simulating chloride ion ingress in concrete [11–13]. In CA modeling, the material domain is discretized into a lattice of cells, each evolving according to predefined local interaction rules. Through simple local evolution mechanisms, complex global diffusion behavior can be reproduced without relying on analytical solutions or strong homogenization assumptions. Early applications of CA methods fo-

cused on simulating chloride ingress in reinforced concrete structures at the structural scale, demonstrating their capability to predict time-dependent chloride concentration distributions under varying environmental and material conditions [14]. Subsequently, spatially irregular and three-dimensional CA models were developed to incorporate both diffusion driven by concentration gradients and permeation driven by pressure gradients, with simulated results showing good agreement with experimental measurements and field data [15]. More recent studies have advanced toward mesoscopic CA models that explicitly account for aggregate distribution, moisture transport, chloride diffusion, and binding effects. By introducing refined cell state variables and evolution rules, these models provide an improved description of material heterogeneity while maintaining reasonable computational efficiency [10]. Furthermore, multi-factor coupled CA models have been proposed to consider sustained loading, freeze–thaw cycling, and random diffusion behavior, exhibiting improved predictive capability compared with traditional Fick-based models under complex service conditions [16,17].

Based on the CA framework previously established in Ref. [14], which incorporates the effects of spatiotemporal variability, water–binder ratio, and stress state on chloride ingress, this study develops an enhanced CA model to simulate the chloride-induced deterioration process of concrete structures. The effects of mineral admixtures on chloride transport are incorporated through admixture-related transport and resistance parameters, enabling a more comprehensive representation of the modified pore structure, chloride binding capacity, and diffusion behavior of admixture-modified concrete. Model predictions are compared with results from a representative exposure test, demonstrating that the proposed model can reasonably capture the evolution of chloride concentration profiles and is applicable for simulating chloride ingress in concrete containing mineral admixtures.

2. Cellular Automata Modeling of Chloride Diffusion in Concrete

2.1. Implementation of Fick's Second Law Using CA

CA is a discrete dynamical system composed of a large number of cells with finite states, which evolve in discrete time according to predefined local interaction rules. A cellular automaton consists of several fundamental components, including cells, cell space, neighborhood, state variables, local evolution rules, boundary conditions, and initial conditions. In the present study, each cell represents a small material domain within the concrete, and the state variable of a cell is defined as the chloride ion concentration at a given time. The evolution of chloride concentration within the concrete is governed by the interaction between a cell and its neighboring cells, following the principle of mass conservation.

To simulate the chloride ion diffusion process using CA, the local evolution rule proposed by Biondini is adopted and expressed as

$$C(x, t + \Delta t) = \Phi_0 C(x, t) + \sum_{j=1}^{n} \Phi_j C(x_j, t), \quad (1)$$

where $C(x, t + \Delta t)$ denotes the chloride ion concentration of the cell at position x and time $t + \Delta t$; Φ_0 is the influence coefficient that determines the contribution of the cell state at time t to its state at time $t + \Delta t$; Φ_j represents the influence coefficient of the j-th cell within the x-cell domain on the state of that cell at time $t + \Delta t$; and n is the number of neighboring cells in the neighborhood excluding the cell itself.

CA with a Von Neumann neighborhood of radius 1 is adopted to describe the diffusion process of chloride ions in concrete. For depth-wise diffusion analysis, a one-dimensional formulation is employed. The same formulation can be extended to higher spatial dimen-

sions by equally distributing the neighbor weights to all adjacent cells, thereby preserving isotropic diffusion behavior. Let Δx denote the cell size and Δt denote the evolution time step. The local evolution rule for the chloride concentration at position x and time t can be expressed as

$$C(x, t + \Delta t) = \Phi_0 C(x, t) + \Phi_1 C(x - \Delta x, t) + \Phi_2 C(x + \Delta x, t) \quad (2)$$

According to the law of mass conservation and to ensure isotropic diffusion behavior, the coefficients satisfy $\Phi_1 = \Phi_2 = \frac{1-\Phi_0}{2}$; when $\Delta x \to 0$ and $\Delta t \to 0$, Equation (2) can be further derived as

$$\frac{\partial C(x, t)}{\partial t} = D \sum_{j=1}^{d} \frac{\partial^2 C(x, t)}{\partial x^2} \quad (3)$$

where d represents the spatial dimension of the cellular space and D denotes the chloride diffusion coefficient and can be written as

$$D = \frac{1 - \Phi_0}{2} \frac{\Delta x^2}{\Delta t} \quad (4)$$

It can be observed that the governing equation derived from the CA formulation for simulating chloride ion diffusion is mathematically identical to Fick's second law. Therefore, the effects of multiple influencing factors on chloride diffusion can be incorporated by appropriately modifying the evolution parameter in the CA model [14].

Since the updating rule in Equation (2) corresponds to an explicit diffusion scheme, numerical stability requires the weighting coefficients to remain non-negative, i.e., $0 \leq \Phi_0 \leq 1$. Given D, Δx, and Δt, the discretization parameters must satisfy $\frac{D\Delta t}{(\Delta x)^2} \leq \frac{1}{2}$ in the one-dimensional case and $\frac{D\Delta t}{(\Delta x)^2} \leq \frac{1}{4}$ in the two-dimensional case. This stability condition ensures convergence and numerical consistency of the CA evolution.

2.2. CA-Based Chloride Diffusion Model Considering Spatiotemporal Variability, Water–Binder Ratio, and Stress State

Based on the CA framework, a chloride diffusion coefficient considering the coupled effects of stress state, time dependency, and water–binder ratio is introduced as

$$D = F(t, W/C, \sigma) D_0 \quad (5)$$

where $F(t, W/C, \sigma) = (\frac{t_0}{t})^{(2.5W/C - 0.6)}(1 + A_1\sigma + A_2)$, while A_1 and A_2 are stress influence coefficients.

By combining the chloride diffusion coefficient derived from the CA model (Equation (4)) with the diffusion coefficient accounting for stress state, time dependency, and water–binder ratio (Equation (5)), the evolution parameter of chloride ingress under multi-factor coupling can be obtained as

$$\Phi_0 = 1 - \frac{2d\Delta t(\frac{t_0}{t})^{(2.5W/C - 0.6)}(1 + A_1\sigma + A_2\sigma^2) D_0}{(\Delta x)^2} \quad (6)$$

By specifying the initial conditions, boundary conditions, evolution parameters, and evolution time steps according to the environmental exposure conditions of concrete structures, the chloride ingress process under coupled multi-factor effects can be simulated using the proposed CA model.

2.3. CA Model for Chloride Ion Diffusion in Concrete with Mineral Admixtures

To incorporate the influence of mineral admixtures into the CA model, the time-dependent diffusion formulation adopted in Ref. [14] is extended by explicitly linking the evolution parameter to mixture composition. In Ref. [14], the diffusion coefficient follows the model proposed by Thomas [18] to describe time dependency:

$$D(t) = D_0 \cdot (\frac{t_0}{t})^m \tag{7}$$

where m is a constant dependent on the concrete composition.

Based on the model proposed by Mangat and Molloy [19], Ref. [14] adopts a fixed value of m, $m = 2.5W/C - 0.6$. The magnitude of m governs the diffusion rate, and the constituent materials of concrete significantly affect the chloride diffusion behavior. The influence of mineral admixtures on chloride diffusion in concrete is explicitly considered, the parameter m is determined using the empirical formula provided in the Life-365 version 1.0 software developed in the United States [20]:

$$m = 0.2 + 0.4(F/50 + K/70) \tag{8}$$

where F is the percentage of fly ash content and K is the percentage of slag content.

Substituting Equation (8) into Equation (7), Equation (7) can be rewritten as

$$D(t) = D_0 \cdot (\frac{t_0}{t})^{0.2+0.4(F/50+K/70)} \tag{9}$$

The chloride diffusion coefficient of concrete containing mineral admixtures under multi-factor coupling conditions can be expressed as

$$D(t) = D_0 \cdot (\frac{t_0}{t})^{0.2+0.4(F/50+K/70)}(1 + A_1\sigma + A_2\sigma^2) \tag{10}$$

where D_0 denotes the chloride diffusion coefficient at time t_0.

By combining Equation (10) with Equation (4), the evolution parameter for chloride ingress in admixture-modified concrete under multi-factor coupling can be obtained as

$$\Phi_0 = 1 - \frac{2d\Delta t(\frac{t_0}{t})^{0.2+0.4\ F/50+K/70)}(1 + A_1\sigma + A_2\sigma^2)D_0}{(\Delta x)^2} \tag{11}$$

In numerical implementation, the evolution parameter defined in Equation (11) governs the rate and characteristics of chloride transport within the CA model. In contrast to formulations that employ a fixed or solely time-dependent diffusion parameter, the present evolution parameter integrates time dependency, mineral admixture content, stress state, and water–binder ratio into a unified representation of transport behavior. Once the mineral admixture proportions and the initial diffusion coefficient D_0 are specified, the corresponding time-dependent diffusion coefficient can be evaluated, and the evolution parameter is determined accordingly. The cellular space is discretized in accordance with the cross-sectional geometry of the concrete member, and the evolution rule is implemented through a MATLAB-based computational program. Cells located outside the structural domain are assigned zero concentration, while boundary cells are prescribed with the corresponding surface chloride concentrations. During the discrete evolution process, chloride concentration is updated locally according to the predefined interaction rule, leading to a progressive redistribution of concentration in space and time. Through this procedure, the CA framework provides a numerical realization of chloride ingress in concrete containing mineral admixtures under coupled multi-factor effects.

3. Model Validation

Long-term field exposure tests conducted by Thomas and Bamforth [18] are adopted to validate the proposed CA model. Eighteen reinforced concrete specimens with dimensions of 1.0 m × 0.5 m × 0.3 m were cast on site in 1987 and exposed to the tidal splash zone along the southeast coast of the United Kingdom. Three concrete types were investigated: a control mix containing only Portland cement (PC), a mix incorporating 30% fly ash as partial cement replacement (fly ash concrete), and a mix incorporating 70% ground granulated blast-furnace slag as partial cement replacement (slag concrete). For the PC, the mixture consisted of 288 kg/m^3 of Portland cement, 190 kg/m^3 of water, 660 kg/m^3 of sand, and 1240 kg/m^3 of coarse aggregate, corresponding to a water–binder ratio of 0.66. For the fly ash concrete, the binder contained 227 kg/m^3 of Portland cement and 98 kg/m^3 of fly ash, along with 170 kg/m^3 of water, 585 kg/m^3 of sand, and 1305 kg/m^3 of coarse aggregate, resulting in a water–binder ratio of 0.54. For the slag concrete, the binder consisted of 110 kg/m^3 of Portland cement and 255 kg/m^3 of ground granulated blast-furnace slag, together with 177 kg/m^3 of water, 600 kg/m^3 of sand, and 1240 kg/m^3 of coarse aggregate, giving a water–binder ratio of 0.48. The corresponding 28-day compressive strengths reported in Ref. [18] were 39.4 MPa for PC, 49.6 MPa for fly ash concrete, and 37.9 MPa for slag concrete, respectively. During the exposure period, chloride ion concentrations at various depths were measured at different exposure ages. The experimentally measured surface chloride concentrations and apparent diffusion coefficients reported in Ref. [18] are adopted as prescribed boundary and transport parameters. In the simulations, a Dirichlet boundary condition is imposed at the exposed surface by prescribing the measured surface chloride concentration. The spatial discretization is selected to be consistent with the experimental depth interval to enable direct comparison between simulated and measured concentration profiles. Time advances in discrete evolution steps, with one evolution step corresponding to 0.25 years of exposure. The selected discretization parameters satisfy the stability condition derived in Section 2.1. By adopting experimentally determined boundary and transport parameters, environmental variability is effectively minimized, allowing the validation to focus specifically on evaluating the effectiveness of the CA evolution rules and the multi-factor coupling framework in characterizing the internal migration process of chloride ions. The simulated chloride concentration profiles are then compared with the measured values at corresponding depths and exposure times to assess the applicability and reliability of the proposed model.

3.1. Comparison Results for Fly Ash Concrete

In Ref. [18], the fly ash replacement ratio was 30%. The chloride ion concentration distributions obtained from the CA simulations at different exposure times are illustrated in Figure 1.

As shown in Figure 1, chloride ions gradually diffuse into the interior of the concrete with increasing exposure time, resulting in a continuous increase in penetration depth. Meanwhile, the surface chloride ion concentration (C_s) also increases progressively. A comparison between the CA simulated results and the experimental data is presented in Table 1. To quantitatively evaluate the predictive accuracy of the proposed CA model, the root mean square error (RMSE) is calculated at each exposure age based on the chloride concentration differences between experimental and simulated values at all measured depths. The RMSE is defined as:

$$RMSE = \sqrt{\frac{1}{n}\sum_{i=1}^{n}(C_i^{CA} - C_i^{\exp})^2} \quad (12)$$

where C_i^{CA} and C_i^{exp} represent the simulated and experimental chloride concentrations at each depth, respectively, and n is the number of measurement points.

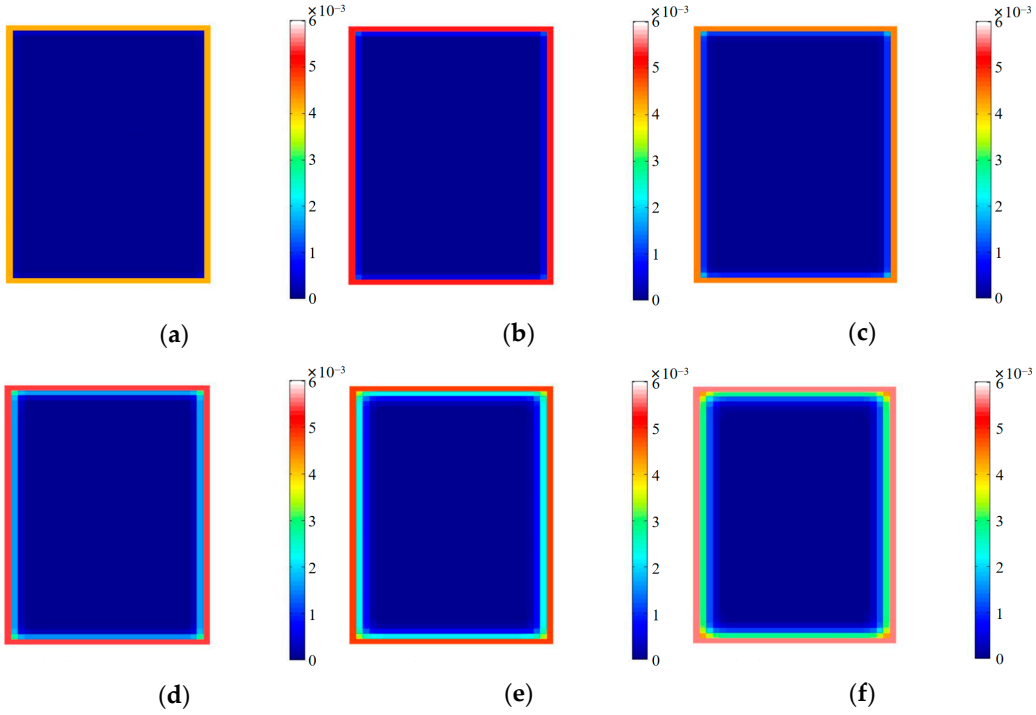


Figure 1. Chloride ion penetration process in fly ash concrete (unit: kg/m^3). (**a**) 0.5 years; (**b**) 1 year; (**c**) 2 years; (**d**) 3 years; (**e**) 6 years; (**f**) 8 years.

Table 1. Experimental and CA-simulated results for fly ash concrete under field exposure.

Exposure Time	C_s (kg/m^3)	Depth (mm)	D ($\times 10^{-12}$ m^2/s)	Φ_0	C^{exp} (kg/m^3)	C^{CA} (kg/m^3)	RMSE ($\times 10^{-4}$)
0.5 years	0.42	0–10	4.3	0.85395	0.0028	0.0004	11.036
		10–20			0.00087	0.0003	
		20–30			0.00007	0	
		30–40			0	0	
		40–50			0	0	
1 year	0.53	0–10	2	0.91098	0.00427	0.0012	13.821
		10–20			0.00097	0.0007	
		20–30			0.0001	0.0001	
		30–40			0.00023	0	
		40–50			0	0	
2 years	0.45	0–10	1.9	0.97229	0.00333	0.0018	7.266
		10–20			0.0016	0.0011	
		20–30			0.00037	0.0002	
		30–40			0.0001	0	
		40–50			0.0001	0	
3 years	0.54	0–10	1.1	0.98748	0.00383	0.0028	4.700
		10–20			0.00173	0.0018	
		20–30			0.00013	0.0003	
		30–40			0.0001	0.0001	
		40–50			0.0001	0	

Table 1. *Cont.*

Exposure Time	C_s (kg/m^3)	Depth (mm)	D ($\times 10^{-12}$ m^2/s)	Φ_0	C^{exp} (kg/m^3)	C^{CA} (kg/m^3)	RMSE ($\times 10^{-4}$)
6 years	0.48	0–10	0.81	0.99254	0.00367	0.0034	3.376
		10–20			0.00193	0.0013	
		20–30			0.0001	0.0004	
		30–40			0.0001	0.0001	
		40–50			0.0001	0	
8 years	0.56	0–10	0.59	0.99631	0.00419	0.0043	4.495
		10–20			0.00308	0.0021	
		20–30			0.00057	0.0007	
		30–40			0.00012	0.0002	
		40–50			0.00012	0	

It can be observed that the chloride ion concentration decreases with increasing depth. With increasing exposure time, the chloride ion penetration depth increases continuously. As shown in Table 1, the RMSE decreases from 11.036 $\times$ 10^{-4} at 0.5 years to 7.266 $\times$ 10^{-4} at 2 years, indicating a progressive improvement in prediction accuracy with increasing exposure time. Although relatively larger deviations are observed at early ages, the RMSE values at medium-to-long exposure durations remain comparatively low, demonstrating that the CA model is capable of reasonably capturing the evolution of chloride concentration profiles in fly ash concrete.

3.2. Comparison Results for Slag Concrete

For slag concrete, the replacement ratio of slag in Ref. [18] was 70%. The simulated chloride ingress process of slag concrete at different exposure ages is shown in Figure 2.

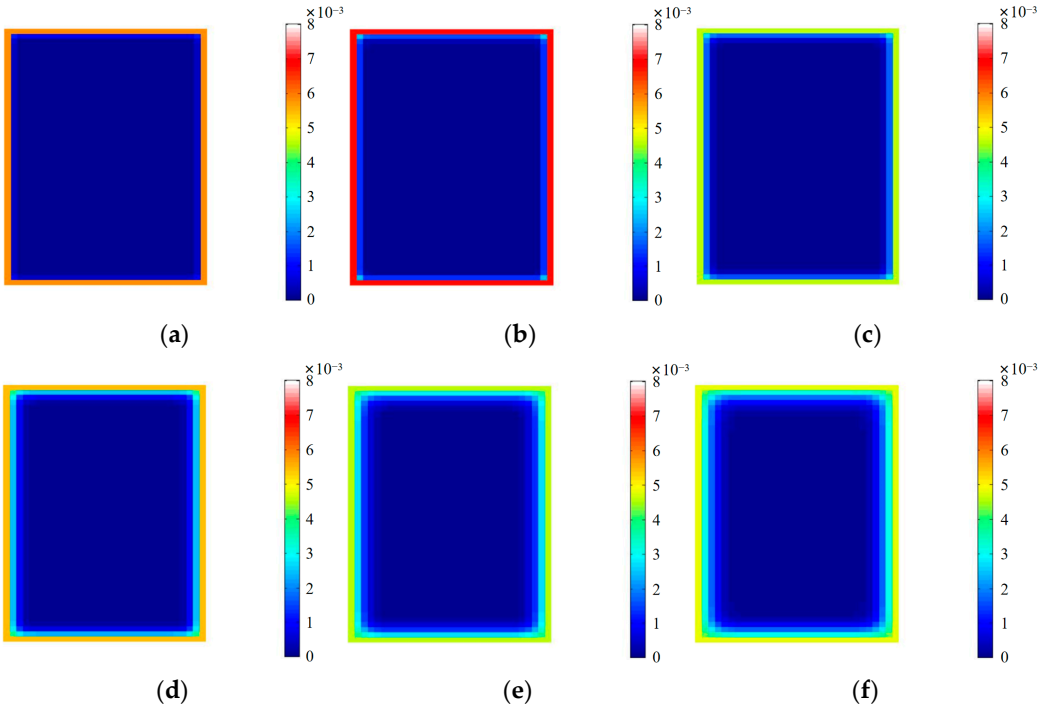


Figure 2. Chloride ion penetration process in slag concrete (unit: kg/m^3). (**a**) 0.5 years; (**b**) 1 year; (**c**) 2 years; (**d**) 3 years; (**e**) 6 years; (**f**) 8 years.

The comparison between the simulated results and the experimental data is summarized in Table 2. The prediction accuracy for slag concrete is evaluated using the

RMSE values based on Equation (12), as presented in Table 2. The RMSE decreases from 16.353×10^{-4} at 0.5 years to 0.820×10^{-4} at 3 years and remains relatively low at later exposure ages. This quantitative evaluation confirms that the CA model provides satisfactory agreement with experimental measurements, particularly at exposure durations exceeding 2 years. In addition, Table 3 indicates that the penetration depth of slag concrete reaches 50 mm after 2 years of exposure, which is greater than that of fly ash concrete under the same exposure duration, as shown in Table 1.

Table 2. Experimental and CA simulated results for slag concrete under field exposure.

Exposure Time	C_s (kg/m^3)	Depth (mm)	D ($\times 10^{-12}$ m^2/s)	Φ_0	C^{exp} (kg/m^3)	C^{CA} (kg/m^3)	RMSE ($\times 10^{-4}$)
0.5 years	0.58	0–10	7.5	0.71538	0.00437	0.0012	16.353
		10–20			0.00173	0.0001	
		20–30			0.00077	0	
		30–40			0.00027	0	
		40–50			0	0	
1 year	0.68	0–10	2.9	0.83887	0.00493	0.0026	12.330
		10–20			0.0014	0.0004	
		20–30			0.0009	0.0001	
		30–40			0.00073	0	
		40–50			0	0	
2 years	0.46	0–10	1.9	0.96136	0.0034	0.0027	5.270
		10–20			0.00173	0.0008	
		20–30			0.00023	0.0001	
		30–40			0.0001	0.0001	
		40–50			0.00013	0	
3 years	0.54	0–10	0.99	0.91407	0.00387	0.0038	0.820
		10–20			0.00153	0.0015	
		20–30			0.00027	0.0004	
		30–40			0.00013	0.0001	
		40–50			0.0001	0	
6 years	0.46	0–10	1	0.9876	0.00363	0.0038	2.257
		10–20			0.00227	0.0023	
		20–30			0.00067	0.0011	
		30–40			0.0004	0.0004	
		40–50			0.0003	0.0001	
8 years	0.48	0–10	0.63	0.99313	0.00381	0.0042	5.781
		10–20			0.00216	0.0029	
		20–30			0.00068	0.0016	
		30–40			0.00035	0.0007	
		40–50			0.00035	0.0003	

Table 3. RMSE of predicted chloride concentrations at different depth ranges and exposure ages.

RMSE ($\times 10^{-4}$)		Exposure Time					
		0.5 Years	1 Year	2 Years	3 Years	6 Years	8 Years
Fly ash concrete	0–20 mm	17.443	21.792	11.382	7.300	4.847	6.973
	20–50 mm	0.404	1.323	1.277	1.139	1.826	1.121
Slag concrete	0–20 mm	25.205	17.929	8.231	0.539	1.221	5.915
	20–50 mm	4.711	6.253	1.061	0.963	2.738	5.690

3.3. Comparative Analysis of Experimental and Simulated Results

Based on the results presented in Tables 1 and 2, it can be observed that the experimental data obtained after more than 2 years of exposure exhibit agreement with the simulated

results, whereas noticeable discrepancies exist at shorter exposure durations. The RMSE values were additionally calculated for 0–20 mm and 20–50 mm depth ranges respectively at each exposure age, as summarized in Table 3. The RMSE evaluation provides a clearer comparison of the near-surface and deeper regions. For fly ash concrete, the RMSE values within the 0–20 mm range are consistently higher than those within the 20–50 mm range at each exposure time. For example, at 0.5 years, the RMSE in the 0–20 mm range is 17.443×10^{-4}, whereas it is only 0.404×10^{-4} in the 20–50 mm range. A similar trend is observed at other exposure time, where the RMSE beyond 20 mm remains significantly lower than that of the near-surface region. For slag concrete, although relatively higher deviations are observed at early exposure stages, the RMSE values in both depth ranges decrease markedly after 2 years of exposure. For example, at 3 years, the RMSE values are 0.539×10^{-4} for the 0–20 mm range and 0.963×10^{-4} for the 20–50 mm range, both remaining at a relatively low level. Although minor fluctuations between depth ranges can be observed at certain exposure ages, the overall RMSE trend indicates that prediction errors in the deeper region are generally reduced after medium-to-long exposure durations.

Overall, these quantitative results confirm that the CA model exhibits improved agreement with experimental measurements at depths greater than 20 mm, while differences are more evident within the first 20 mm. The discrepancies between the experimental and simulated results can be attributed to the following factors. First, a portion of chloride ions present in concrete may originate from raw materials used during casting, such as natural aggregates, mixing water, and chemical admixtures, which increases the initial chloride ion content and may not be fully reflected in the model initialization. Second, mineral admixtures such as fly ash or slag are known to enhance the chloride binding capacity of concrete through chemical binding and physical adsorption mechanisms, as reported in previous studies [21–26]. In the present model, chloride binding is not explicitly simulated through a free/bound chloride partition formulation. Instead, the influence of mineral admixtures is incorporated indirectly via the modification of the time-dependent diffusion parameter. Therefore, the binding effect is implicitly reflected in the apparent diffusion behavior rather than explicitly represented. This simplification may contribute to deviations between simulated and measured concentrations, particularly at early exposure stages. Third, as penetration depth increases, chloride ion concentration decreases significantly. Measurements at very low concentration levels are more susceptible to environmental disturbance and operational variability, which may introduce experimental uncertainty. Finally, in the simulation process, the time-dependent evolution of surface chloride concentration and diffusion coefficient is simplified, and interactions between successive exposure periods are not fully incorporated. Therefore, the observed discrepancies between the simulated and experimental results are considered acceptable within the scope of this study.

Based on the comparative analysis of the simulated and experimental results, it can be concluded that the CA model provides a reasonable and feasible approach for simulating the chloride ion diffusion process in concrete containing mineral admixtures. Figure 3 presents the variation in chloride ion concentration with depth for both fly ash concrete and slag concrete under different exposure times, as obtained from field experiments and CA simulations. As shown in Figure 3, when the exposure time exceeds 2 years, a high degree of agreement between the experimental and simulated results is observed. Both experimental and simulated results indicate that, under identical conditions, the chloride ion concentration in slag concrete is higher than that in fly ash concrete. It suggests that fly ash concrete exhibits superior resistance to chloride ion penetration.

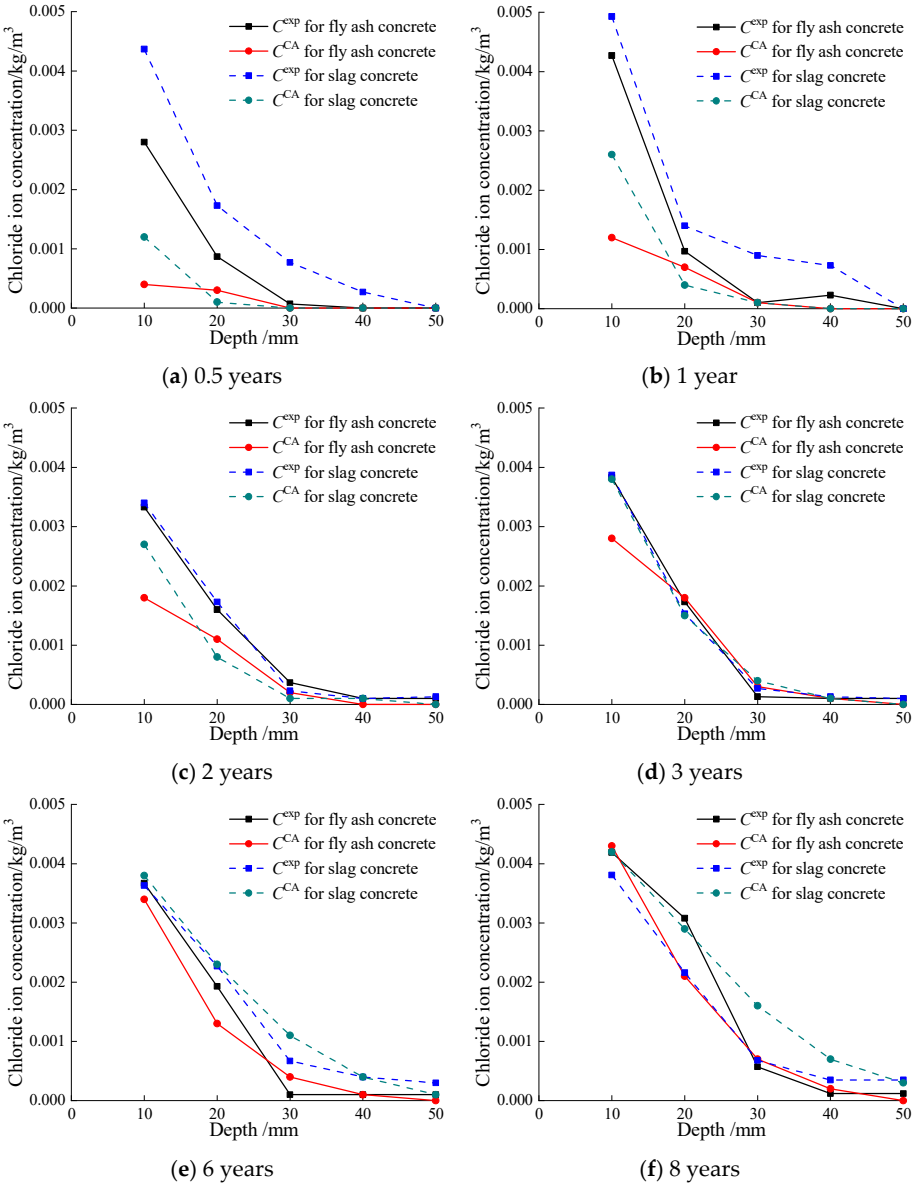


Figure 3. Chloride ion concentration for fly ash and slag concretes at different exposure time.

4. Application Analysis

Taking the reinforced concrete beam tested in Ref. [27] as an example, the CA model is employed to simulate the chloride ion penetration process. The concrete mix proportions used in Ref. [27] are listed in Table 4. The thickness of the concrete cover is 20 mm. The surface chloride ion concentration is assumed to increase with time at a rate of 0.1% per year. The initial surface chloride ion concentration is taken as 0.404 kg/m^3, and the chloride diffusion coefficient is assumed to be 6×10^{-12} m^2/s. The cross-sectional dimensions of the beam are shown in Figure 4.

Table 4. Mixed proportions of concretes.

Specimen	Water–Binder Ratio	Cement (kg/m^3)	Fly Ash (kg/m^3)	Slag (kg/m^3)	Sand (kg/m^3)	Coarse Aggregate (kg/m^3)	Water (kg/m^3)
S30C50	0.35	336	0	144	704	1148	168
S70C50	0.30	156	0	364	693	1131	156

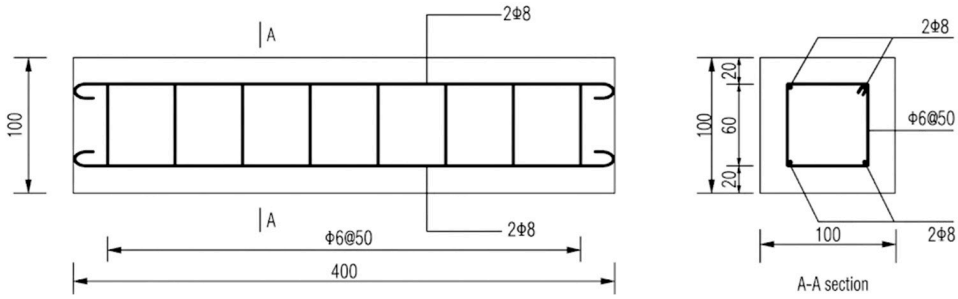
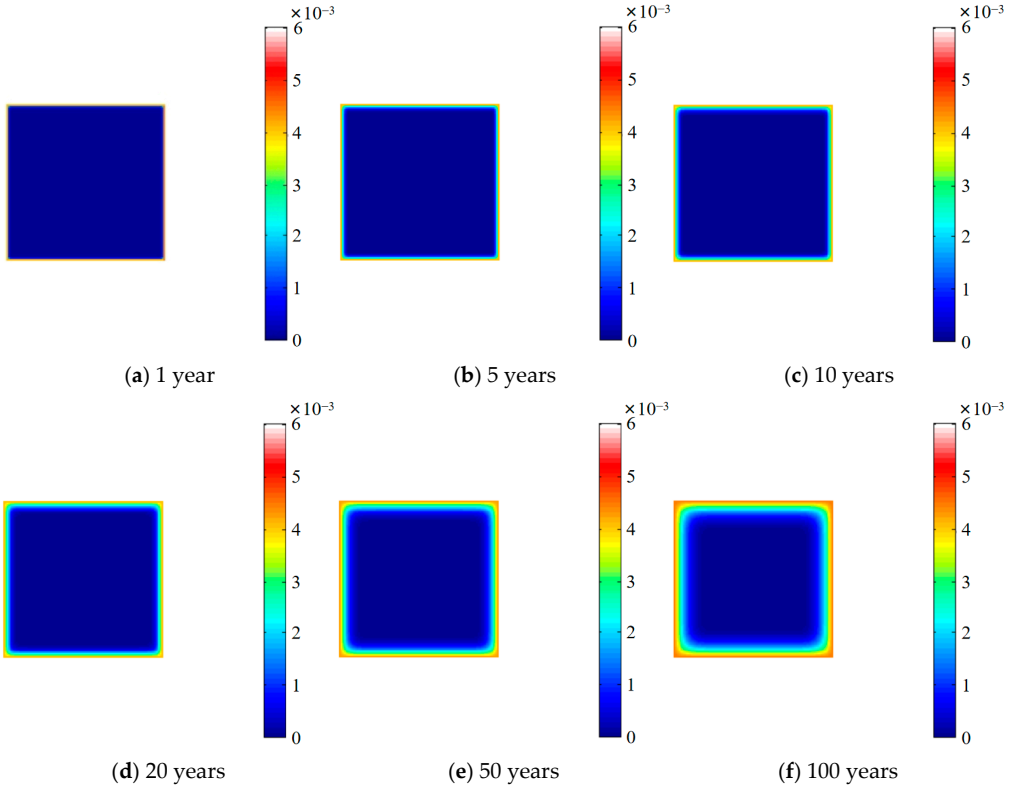


Figure 4. Dimension and reinforcement layout of concrete test beam [27].

The chloride ion penetration behavior of the concrete section is simulated at exposure ages of 1, 5, 10, 20, 50, and 100 years, respectively. The simulated results for the S70C50 specimen are illustrated in Figure 5. As shown in Figure 5, with increasing exposure time, chloride ions gradually diffuse into the interior of the concrete section, while the surface chloride ion concentration increases continuously. Meanwhile, the diffusion rate gradually accelerates. After approximately 50 years of exposure, a rapid increase in chloride concentration near the reinforcement surface is observed.



(**a**) 1 year (**b**) 5 years (**c**) 10 years

(**d**) 20 years (**e**) 50 years (**f**) 100 years

Figure 5. Process of chloride ion penetration of S70C50 concrete beam.

The chloride ion concentration at the reinforcement surface for different slag replacement ratios is shown in Figure 6. As illustrated in Figure 6, for concrete with the same strength grade, the concrete containing 70% slag exhibits better resistance to chloride ion penetration than that containing 30% slag. This indicates that increasing the slag replacement ratio is beneficial for improving the resistance of concrete to chloride ion ingress. This behavior can be attributed to the initial chloride-binding effect of slag. During the hydration process of slag concrete, the generated C-S-H gel is capable of adsorbing a portion of chloride ions, thereby reducing their penetration into the concrete interior. Overall, during the early service stage of concrete, the chloride ion concentration around the reinforcement

remains relatively low. However, after approximately 50 years of exposure, the chloride ion concentration in the vicinity of the reinforcement increases sharply. The accumulation of chloride ions at the reinforcement surface reduces the local alkalinity and may eventually lead to depassivation of the steel reinforcement, thereby increasing the risk of corrosion and degradation of structural load-bearing capacity.

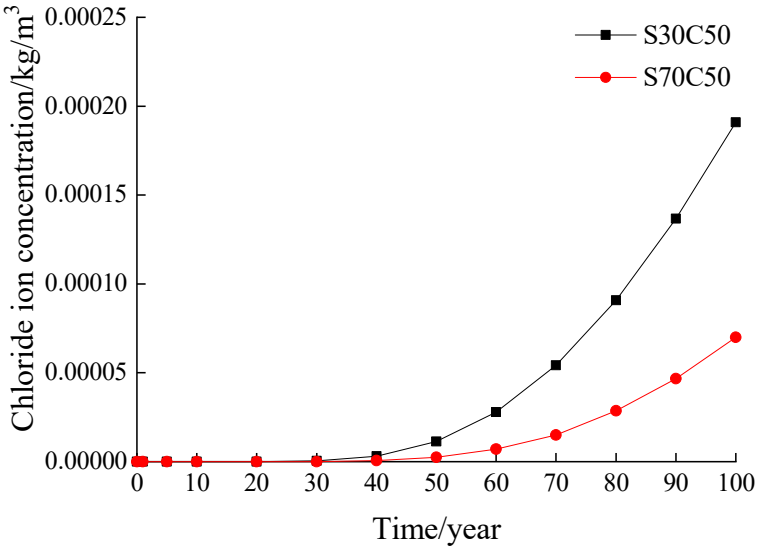


Figure 6. Chloride concentration at the reinforcement surface for different slag replacement ratios.

5. Conclusions

In this study, an improved CA model was developed to simulate the chloride ion diffusion behavior in concrete with mineral admixtures. The model was validated using long-term field exposure data and subsequently applied to reinforced concrete beams. Based on the results and analysis presented in this paper, the following conclusions can be drawn:

(1) An enhanced CA model incorporating the effects of mineral admixture replacement ratio, time dependency, and multi-factor coupling was established to simulate chloride ion diffusion in concrete. The proposed model is capable of capturing the evolution of chloride concentration profiles with exposure time and depth. Model validation results demonstrate that the simulated chloride concentrations show good agreement with experimental measurements, particularly at medium-to-long exposure ages, confirming the reliability and applicability of the improved CA model for admixture-modified concrete.

(2) By explicitly accounting for the influence of mineral admixtures on the chloride diffusion coefficient through an admixture-dependent time evolution parameter, the proposed CA model enables a quantitative comparison of chloride resistance among concretes incorporating different types and replacement ratios of mineral admixtures. This feature allows the model to be effectively used as a numerical tool for evaluating and comparing the chloride ingress resistance of concrete mixtures under varying material compositions.

(3) The application analysis of a reinforced concrete beam indicates that chloride ions continuously penetrate from the concrete surface toward the interior with increasing service time, leading to a progressive increase in chloride concentration at the reinforcement surface. The simulated results reveal that the chloride concentration near the reinforcement remains relatively low during the early service stage, whereas a pronounced increase occurs after approximately 50 years of exposure, implying a

significantly elevated risk of steel depassivation and corrosion initiation in the later service life.

(4) Under comparable strength conditions, increasing the slag replacement ratio enhances the resistance of concrete to chloride ion ingress. Concrete containing a higher proportion of slag exhibits lower chloride concentrations at the reinforcement surface over the same exposure duration. This improvement can be interpreted as being associated with pore structure refinement and the enhanced chloride binding capacity of slag hydration products, which are indirectly reflected in the modified diffusion parameter adopted in the present model.

Author Contributions: Conceptualization, J.D. and J.Z.; methodology, J.D. and J.Z.; software, J.D. and Y.Z.; validation, J.D.; data curation, J.D. and Q.M.; writing—original draft preparation, J.D. and Y.Z.; visualization, A.C. and Y.Z.; supervision, J.Z. and Q.M.; project administration, J.D. and J.Z.; funding acquisition, J.D. All authors have read and agreed to the published version of the manuscript.

Funding: This research was funded by Department of Science and Technology Shandong Province (grant number ZR2024QE376 and 2024CXGC010321) and Shandong Key Laboratory of Civil Engineering Disaster Prevention and Mitigation (Shandong University of Science and Technology) (grant number CDPM2023KF10).

Institutional Review Board Statement: No applicable.

Informed Consent Statement: No applicable.

Data Availability Statement: The original contributions presented in this study are included in the article. Further inquiries can be directed to the corresponding authors.

Conflicts of Interest: Author Ankai Cao was employed by the company State Grid Shandong Integrated Energy Services Co., Ltd. The remaining authors declare that the research was conducted in the absence of any commercial or financial relationships that could be construed as a potential conflict of interest.

References

1. Xu, Q.; Liu, B.; Dai, L.; Yao, M.; Pang, X. Factors Influencing Chloride Ion Diffusion in Reinforced Concrete Structures. *Materials* **2024**, *17*, 3296. [CrossRef] [PubMed]
2. Chen, F.; Zhang, Y.; Huang, Y.; Su, Y. Mesoscale Numerical Model of Chloride Ion Diffusion through Concrete under Wet-Dry Cycles Considering Multiple Factors. *J. Build. Eng.* **2025**, *114*, 114276. [CrossRef]
3. Feng, T.; Miao, Y.; Tan, Y.; Yang, Z.; Cao, T.; Wang, F.; Jiang, J. Prediction Methodology for the Service Life of Concrete Structures in Marine Environment: From Materials to Performance. *Engineering* 2025, *in press*. [CrossRef]
4. Zhang, H.; Zgao, M.; Song, L.; Yang, Y.; He, J. The Evolution of Concrete Microstructure and Chloride-Ion Diffusion Coefficient under Cyclic Axial Compression. *Int. J. Concr. Struct. Mater.* **2025**, *19*, 56. [CrossRef]
5. Jin, H.; Liu, J.; Zhong, D.; Tang, L. Experimental Study on Chloride Ion Diffusion Behavior and Microstructure in Concrete under Alternating Ambient Humidity Conditions. *Constr. Build. Mater.* **2023**, *401*, 132886. [CrossRef]
6. Ji, Z.; Peng, B.; Guo, W.; Sun, M. Simulation of Macroscopic Chloride Ion Diffusion in Concrete Members. *Coatings* **2025**, *15*, 1131. [CrossRef]
7. Jeon, S.-M.; Liyew, G.; Kim, H.-K. Service Life Assessment of Accelerated Carbonation-Cured Concrete Considering Weathering Carbonation and Chloride Ingression. *J. Build. Eng.* **2025**, *103*, 112094. [CrossRef]
8. Wang, H.; Wen, B.; Xu, P.; Zhang, L.; Niu, D.; Berardi, M. Study on Chloride Ion Diffusion Behavior of Waste Glass Concrete under Carbonation and Chloride Corrosion. *Case Stud. Constr. Mater.* **2025**, *23*, e05309. [CrossRef]
9. Tang, H.; Yang, Y.; Peng, J.; Liu, P.; Zhang, J. Test and Mesoscopic Analysis of Chloride Ion Diffusion of High-Performance Concrete with Fly Ash and Silica Fume. *Coatings* **2022**, *12*, 1095. [CrossRef]
10. Ruan, X.; Li, Y.; Zhou, X.; Jin, Z.; Yin, Z. Simulation Method of Concrete Chloride Ingress with Mesoscopic Cellular Automata. *Constr. Build. Mater.* **2020**, *249*, 118778. [CrossRef]
11. Al-samawi, M.; Zhu, J.; Rong, W. Application of 3D cellular automata-based analysis to chloride diffusion process in concrete bridges. *Structures* **2023**, *47*, 500–519. [CrossRef]
12. Zhu, J.; He, L. Cellular automata-based chloride ion diffusion simulation of concrete bridges under multi-factor coupling actions. *J. Wuhan Univ. Technol. Mater* **2012**, *27*, 160–165. [CrossRef]

13. Wang, Y.; An, M.; Yu, Z.; Han, B.; Ji, W. Experimental and cellular-automata-based analysis of chloride ion diffusion in reactive powder concrete subjected to freeze-thaw cycling. *Constr. Build. Mater.* **2018**, *172*, 760–769. [CrossRef]
14. Zhu, J.; Shi, X.; He, L. Cellular Automata-based Model for Simulating the Chloride Ion Penetration Process of Concrete Bridge. *J. Basic Sci. Eng.* **2013**, *21*, 127–136. (In Chinese)
15. Xiang, Y.; Wu, Q. Simulation and analysis of the chloride ions diffusion and penetration effect in concrete based on cellular automata. *China Civ. Eng. J.* **2015**, *48*, 36–43. (In Chinese)
16. Ma, J.; Lin, P. Simulation approach for random diffusion of chloride in concrete under sustained load with cellular automata. *Materials* **2022**, *15*, 4384. [CrossRef]
17. Zhu, J.; Al-samawi, M.; Yang, Y.; Al-Shakhdha, N.A. An approach for simulating and evaluating the effect of sulfate attack on the durability of concrete bridges based on a three-dimensional cellular automata model. *Eng. Struct.* **2023**, *291*, 116451–116468. [CrossRef]
18. Thomas, M.D.A.; Bamforth, P.B. Modelling chloride diffusion in concrete: Effect of fly ash and slag. *Cem. Concr. Res.* **1999**, *29*, 487–495. [CrossRef]
19. Mangat, P.S.; Molloy, B.T. Prediction of long-term chloride concentration in concrete. *Mater. Struct.* **1994**, *27*, 338–346. [CrossRef]
20. Thomas, M.D.A.; Bentz, D. Life-365: Computer program for predicting the service life and life-cycle costs of reinforced concrete structures exposed to chlorides. In *User Manual (Version 1.0)*; Nordic Mini Seminar & Fib TG: Göteborg, Sweden, 2001; Volume 5.
21. Yuan, Q.; Shi, C.; De Schutter, G.; Audenaert, K.; Deng, D. Chloride binding of cement-based materials subjected to external chloride environment: A review. *Constr. Build. Mater.* **2009**, *23*, 1–13. [CrossRef]
22. Lv, J.; Li, D.; Yang, X.; Rong, H.; Xian, C.; Zhang, Z.; Huang, W.; Li, S. Chloride ion binding in cementitious materials: A review of influencing factors and control methods. *Case. Stud. Constr. Mat.* **2025**, *22*, e04201. [CrossRef]
23. Zhao, Y.; Hu, X.; Shi, C.; Yuan, Q.; Zhu, D. Determination of free chloride in seawater cement paste with low water–binder ratio. *Cem. Concr. Compos.* **2021**, *124*, 104217. [CrossRef]
24. Zhao, Y.; Hu, X.; Li, H.; Tavio, T.; Shi, C. Factors affecting free chloride contents of hardened cement paste with a low water-to-binder ratio determined by rapid water extraction. *Cem. Concr. Compos.* **2024**, *148*, 105491. [CrossRef]
25. De Weerdt, K.; Colombo, A.; Coppola, L.; Justnes, H.; Geiker, M.R. Impact of the associated cation on chloride binding of Portland cement paste. *Cem. Concr. Res.* **2015**, *68*, 196–202. [CrossRef]
26. Georget, F.; Babaahmadi, A.; Machner, A.; Mrak, M.; Dolenec, S.; Xiong, Q.X.; Shiju, J.; Snoeck, D.; Suraneni, P.; Wilson, W. Measuring chloride binding in cementitious materials: A review by RILEM TC 298-EBD. *Mater. Struct.* **2025**, *58*, 348. [CrossRef]
27. Wu, Q. Durability and Service Life Prediction of Reinforced Concrete Flexural Members in Marine Environment. Ph.D. Dissertation, Nanjing University of Aeronautics and Astronautics, Nanjing, China, 2010. (In Chinese)

Disclaimer/Publisher's Note: The statements, opinions and data contained in all publications are solely those of the individual author(s) and contributor(s) and not of MDPI and/or the editor(s). MDPI and/or the editor(s) disclaim responsibility for any injury to people or property resulting from any ideas, methods, instructions or products referred to in the content.